Pd–Pt random alloy nanocubes with tunable compositions and their enhanced electrocatalytic activities†

Qiang Yuan,[ab] Zhiyou Zhou,*[c] Jing Zhuang[a] and Xun Wang*[a]

Received (in Cambridge, UK) 30th October 2009, Accepted 7th December 2009
First published as an Advance Article on the web 5th January 2010
DOI: 10.1039/b922792j

Monodisperse, highly-selective sub-10 nm Pd–Pt random alloy nanocubes have been successfully synthesized in aqueous solution, and the electrocatalytic activity of these Pd–Pt alloys towards formic acid oxidation was investigated and compared with the activity of Pd sub-10 nm nanocubes, and the commercial Pd and Pt black.

Recently bimetallic noble metal nanostructures have been attracting extensive interest because of their superior catalytic properties relative to single compositions.[1–6] Previous studies[7–12] have shown that the catalytic activity of bimetallic noble metals highly depends on sizes, shapes, compositions and surface structures. Thus far, the synthesis of bimetallic noble metal nanostructures mainly includes co-deposition of bimetallic precursors on support,[13] co-decomposition/co-reduction in polyol or an oil system[14,15] and the seed-mediated epitaxial growth method,[16,17] *etc*. However, the synthesis of bimetallic alloys with controlled size and shape has had only a limited success. Very recently, Zou and co-workers[11] prepared Pt–Cu alloy nanocubes by co-reduction of $Pt(acac)_2$ and $Cu(acac)_2$ in a 1-octadecene solution in the presence of 1,2-tetradecanediol, tetraoctylammonium bromide, oleylamine and 1-dodecanethiol. Zheng and co-workers[12] reported hollow Pd/Pt alloy nanocubes in DMF containing PVP and NaI with $Pd(acac)_2$ and $Pt(acac)_2$ as precursors. To the best of our knowledge, the simultaneous composition, shape and size-controlled synthesis of bimetallic alloys based on an aqueous media has not been reported yet to date. In this communication, we report the facile, one-step synthesis of composition-tunable, high-yield PdPt bimetallic random alloy nanocubes (two metals atoms are mixed statistically according to the overall concentration)[18] with diameters within sub-10 nm through an aqueous colloidal method by use of simple inorganic precursors, $PdCl_2$ and K_2PtCl_6; furthermore, the internal composition can be harnessed in a wide range. These alloy nanocubes have shown enhanced and composition-dependent electrocatalytic activity towards formic acid oxidation.

The Pd–Pt alloy nanocubes were synthesized according to our previous method[19] by co-reduction of $PdCl_2$ and K_2PtCl_6 in the presence of sodium lauryl sulfate (SLS), poly(vinyl-pyrrolidone) (PVP, MW = 30 000), and KBr in the aqueous solution (see ESI† for details).

Fig. 1(a)–(c) show the representative transmission electron microscopic (TEM) and HRTEM images of as-synthesized Pd–Pt bimetallic nanocubes (the composition of Pd and Pt for all samples was determined by ICP-OES), which show that the products have high monodispersity and the well-defined shape of nanocubes with an average diameter of 7.1 ± 0.2 nm and the selectivity for nanocubes is more than 90%. Moreover, the nanocubes have a strong tendency to self-assemble into 2D arrays on the TEM grid. Obvious lattice fringes appear on the surface of single cubes, which orient in the same direction (Fig. 1b and Fig. S1, ESI†). The interval between two lattice fringes is examined to be 0.196 nm, close to the (200) lattice spacing of the fcc palladium/platinum. The FT patterns of a single cube are shown in Fig. 1(b) and Fig. S1 (ESI†). The square pattern also indicates the nanocubes have the fcc structure surrounded by (200) facets. As the Pd and Pt have a very small lattice mismatch of only 0.77% and good miscibility, all these factors make the formation of the Pd–Pt alloy possible through a solution route. The techniques of inductively coupled plasma optical emission spectrometry (ICP-OES) and energy-dispersive X-ray spectroscopy (EDS) are often used to characterize the composition of alloys. The results of both ICP-OES and EDS show the nanocubes are made of Pd and Pt (Fig. S1 and Table S1, ESI†). The atomic ratios of Pd and Pt are 74.4 and 25.6 atomic%, and 73.5 and 26.5 atomic% respectively, which are very close to the precursor ratio of Pd and Pt, 75.3 and 24.7 atomic%. Moreover, the EDS line scanning profiles (Fig. 1d and Fig. S1, ESI†) across five particles and a single particle also show the nanocubes consist of Pd and Pt. The XRD results (Fig. S2, ESI†) show the typical fcc structure of palladium/platinum. No single-component peak from palladium or platinum was detected, thus implying the presence of only PdPt alloy single-crystal. However, the (111) peak is stronger than the (200) peak. This is considered the three-dimensional randomly oriented assembly.[19,20]

The variation in morphology and size of the nanocubes did not occur with the change in the quantity of K_2PtCl_6 (Fig. 1a–c and Fig. S1, ESI†). The results of ICP-OES and EDS show that all samples are made of Pd and Pt (Fig. S1 and Table S1, ESI†). Fig. 2(a) shows the comparison of theoretical Pt content with the Pt content from ICP-OES. It shows the atomic ratio of Pt varies regularly. The values from ICP-OES are almost consistent with the theoretical values of Pt precursors below 24.7 atomic% (Table S1, ESI†). When the Pt content is beyond 24.7 atomic%, the experimental values are a

[a] *Department of Chemistry, Tsinghua University, Beijing, 100084, P. R. China. E-mail: wangxun@mail.tsinghua.edu.cn; Tel: 8610 62792791*
[b] *Department of Chemistry, Guizhou University, Guiyang Guizhou, 550025, P. R. China*
[c] *Department of Chemistry, College of Chemistry and Chemical Engineering, Xiamen University, 361005, P. R. China. E-mail: zhouzy@xmu.edu.cn*

† Electronic supplementary information (ESI) available: Experimental details; TEM, HRTEM, EDS profiles, CVs and tables. See DOI: 10.1039/b922792j

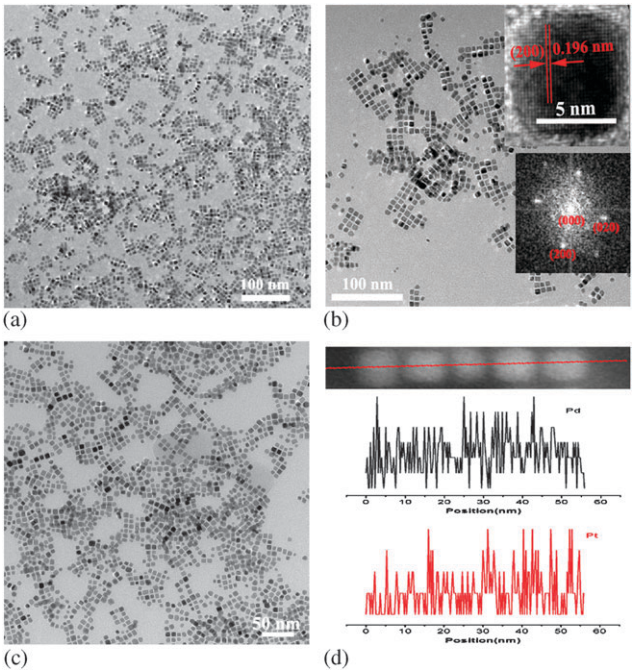

Fig. 1 TEM images of representative Pd–Pt nanocube alloys (a) $Pd_{80.8}Pt_{19.2}$, (b) $Pd_{74.4}Pt_{25.6}$, (c) $Pd_{66.0}Pt_{34.0}$. (The inset is HRTEM and FT patterns of a single nanocube.) (d) The STEM and EDS line scanning profiles of $Pd_{74.4}Pt_{25.6}$ nanocube alloy.

little lower than the theoretical values. This implies that there is preferential reduction of Pd in our system. To verify this hypothesis, we did reference experiments under the same conditions as for the synthesis of Pd–Pt alloy nanocubes except without $PdCl_2$. Unexpectedly, the products of Pt could not be obtained. Therefore, the formation of the PdPt nanocubes alloy is determined by the initial reduction of Pd^{2+}. In our system, we suggest that the Pd–Pt nanocubes alloy is a random alloy (two metals atoms are mixed statistically according to the overall concentration), not a non-random alloy (*e.g.* core@shell-structured alloy) or a phase segregation alloy. Fig. 2(b) shows the XPS data of Pd and Pt of Pd–Pt nanocubes alloys. The binding energy of $Pd3d_{5/2}$ and $Pt4f_{7/2}$ is 335.1 and 70.6 eV respectively. The surface atomic% of Pd and Pt, calculated according to XPS, which is consistent with that from ICP-OES, and the regular variation in the relative intensity of Pd and Pt support the suggestion (Fig. 2a and Table S1, ESI†). Furthermore, the results of EDS, ICP-OES and the EDS line scanning also support the suggestion of Pd–Pt random alloy.

The catalytic activity of Pd–Pt nanocubes alloy towards formic acid oxidation was tested. The electrodes were immersed in a nitrogen-saturated 0.1 M H_2SO_4 solution, and the potential was scanned from 0.05 to 1.1 V (*vs.* reversible hydrogen electrode, RHE) at a scan rate of 50 mV s^{-1} to obtain the cyclic voltammograms (CVs) (Fig. 3 and Fig. S3, ESI†). The hydrogen adsorption/desorption electric charges calculated from the CVs were used to estimate the electrochemically active surface area (ECSA) of the catalysts. For comparison, Pd nanocubes (Fig. S1†), and the commercial Pd black and Pt black were also tested. The CVs of the Pd–Pt alloys show similar shape to that of the Pd nanocubes and

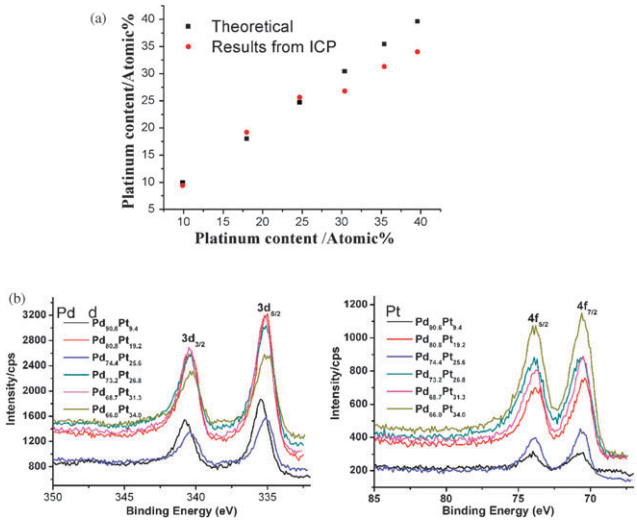

Fig. 2 (a) Comparison of the theoretical Pt content and the Pt content from ICP-OES. (b) Pd and Pt XPS spectra of Pd–Pt nanocubes alloys.

commercial Pd black. However, the hydrogen oxidation peak at 0.1 V gradually disappeared with the increase in Pt content. Finally, the peak fully disappeared when the Pt content increased to 34.0 atomic%. It indicates the surface structure of the catalysts changed owing to the composition variation of the Pd–Pt alloy. These CVs also offer evidence for the suggestion of a Pd–Pt random alloy.

The electrocatalytic activities of the catalysts were tested in the 0.1 M HCOOH + 0.1 M H_2SO_4 solution at a scan rate of 50 mV s^{-1} from 0.05 to 1.1 V. The current density (J) was calculated according to the corresponding surface area measured from the hydrogen adsorption/desorption CVs. Fig. 4(a) and Fig. S4, ESI†, show the comparison of the electrocatalytic properties of the Pd–Pt nanocubes alloys, Pd nanocubes and commercial Pd black. The peak potential and current of the commercial Pd black is 0.48 V and 3.0 mA cm^{-2} and that of the Pd nanocubes is 0.52 V and 3.4 mA cm^{-2}, respectively. Whereas, the peak potential decreases with the increase in Pt content (Fig. 4b), the peak currents of all the Pd–Pt nanocubes alloys are higher than that of the Pd

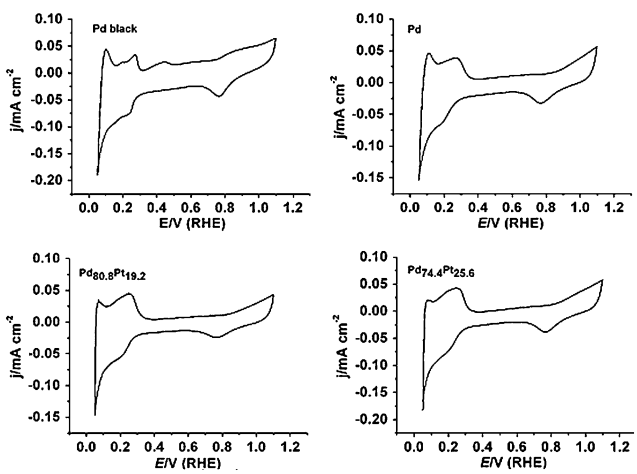

Fig. 3 The cyclic voltammetric curves (CVs) of Pd black, Pd nanocubes and representative nanocubes alloys.

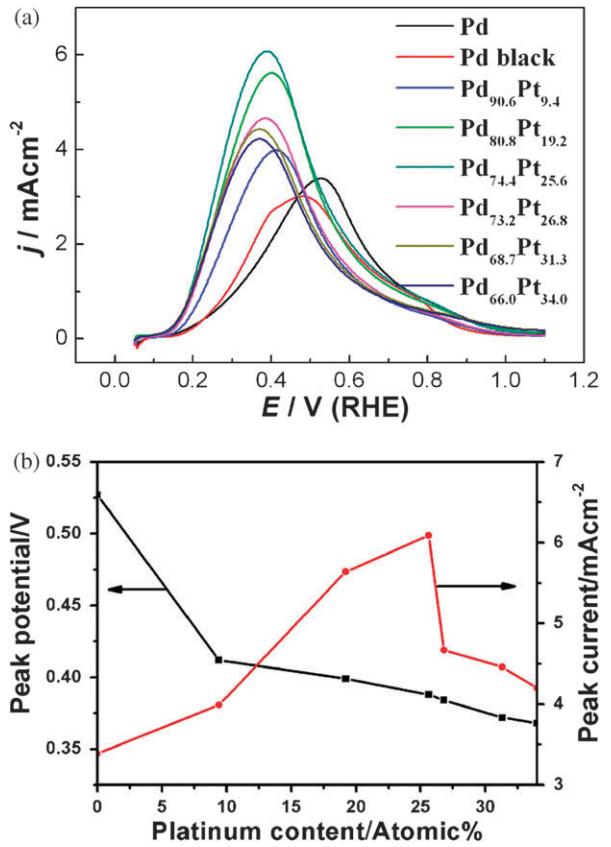

Fig. 4 (a) The comparison of electrocatalytic activities of Pd–Pt nanocubes alloys, Pd nanocubes and commercial Pd black. (b) The dependence of the peak potential and current on Pt content.

nanocubes and commercial Pd black. But the peak current of the Pd–Pt nanocubes alloy increased with the Pt content below 25.6 atomic%, then decreased (Fig. 4b, Table S2, ESI†). For example, the peak potential and current of the typical catalyst, $Pd_{74.4}Pt_{25.6}$ alloy, is 0.39 V and 6.1 mA cm^{-2}, respectively. The maximum of peak potential decrease and peak current increase is 0.11 V and 3.1 mA cm^{-2} compared with the commercial Pd black (Fig. 4b and Table S2, ESI†). Furthermore, the electrocatalytic activity of pure Pt toward formic acid is rather poor as compared to pure Pd or the Pd–Pt alloys (Fig. S4, ESI†). The enhanced electrocatalytic activity of the Pd–Pt nanocubes alloys over pure Pd may be ascribed to the electronic structure modification owing to the presence of Pt at the Pd surface. This phenomenon has also been observed in other bimetallic alloys.[1,2,5]

In conclusion, the composition-tunable, high-selectivity, sub-10 nm Pd–Pt nanocubes with homogenous distribution of Pd and Pt were first successfully synthesized from an aqueous solution. The electrocatalytic activity of these Pd–Pt alloys towards formic acid oxidation was investigated and compared with the activity of Pd sub-10 nm nanocubes and commercial Pd black. The maximum peak current value of the Pd–Pt alloy is two times that of the commercial Pd black, the maximum decrease in peak potential is 0.11 V. This study demonstrates the successful tailoring of electrocatalytic properties of metal nanoparticles by controlling their composition while preserving the same shape and size.

This work was supported by NSFC(20725102, 20921001), the Fok Ying Tung Education Foundation (111012), and the State Key Project of Fundamental Research for Nanoscience and Nanotechnology (2006CB932301).

Notes and references

1 B. Lim, M. Jiang, P. H. C. Camargo, E. C. Cho, J. Tao, X. Lu, Y. Zhu and Y. Xia, *Science*, 2009, **324**, 1302.
2 H. Lee, S. E. Habas, G. A. Somorjai and P. Yang, *J. Am. Chem. Soc.*, 2008, **130**, 5406.
3 Z. Peng and H. Yang, *J. Am. Chem. Soc.*, 2009, **131**, 7542.
4 S. Alayoglu, A. U. Nilekar, M. Mavrikakis and B. Eichhorn, *Nat. Mater.*, 2008, **7**, 333.
5 V. Stamenkovic, B. S. Mun, K. J. J. Mayrhofer, P. N. Ross, N. Markovic, J. Rossmeisl, J. Greeley and J. K. Nskov, *Angew. Chem., Int. Ed.*, 2006, **45**, 2897.
6 M. Saruyama, M. Kanehara and T. Teranishi, *Chem. Commun.*, 2009, 2724.
7 S. Alayoglu, A. U. Nilekar, M. Mavrikakis and B. Eichhorn, *Nat. Mater.*, 2008, **7**, 333.
8 Q. Liu, Z. Yan, N. L. Henderson, J. C. Dauer, D. W. Goodman, J. D. Batteas and R. E. Schaak, *J. Am. Chem. Soc.*, 2009, **131**, 5720.
9 M. Wakisaka, S. Mitsui, Y. Hirose, K. Kawashima, H. Uchida and M. Watanabe, *J. Phys. Chem. B*, 2006, **110**, 23489.
10 Z. Liu, C. Yu, I. Rusakova, A. D. Huang and P. Strasser, *Top. Catal.*, 2008, **49**, 241.
11 D. Xu, Z. Liu, H. Yang, Q. Liu, J. Zhang, J. Fang, S. Zou and K. Sun, *Angew. Chem., Int. Ed.*, 2009, **48**, 4217.
12 X. Huang, H. Zhang, C. Guo, Z. Zhou and N. Zheng, *Angew. Chem., Int. Ed.*, 2009, **48**, 4808.
13 X. Li and I. M. Hsing, *Electrochim. Acta*, 2006, **51**, 3477.
14 Z. Liu, J. E. Hu, Q. Wang, K. Gaskell, A. I. Frenkel, G. S. Jackson and B. Eichhorn, *J. Am. Chem. Soc.*, 2009, **131**, 6924.
15 S. Sun, C. B. Murray, D. Weller, L. Folks and A. Moser, *Science*, 2000, **287**, 1989.
16 F. R. Fan, D. Y. Liu, Y. Wu, S. Duan, Z. X. Xie, Z. Y. Jiang and Z. Q. Tian, *J. Am. Chem. Soc.*, 2008, **130**, 6949.
17 S. E. Habas, H. Lee, V. Radmilovic, G. A. Somorjai and P. D. Yang, *Nat. Mater.*, 2007, **6**, 692.
18 X. Teng, Q. Wang, P. Liu, W. Han, A. I. Frenkel, N. Marinkovic, Hanson and J. C. J. A. Rodriguez, *J. Am. Chem. Soc.*, 2008, **130**, 1093.
19 Q. Yuan, J. Zhuang and X. Wang, *Chem. Commun.*, 2009, 6613.
20 C. Wang, H. Daimon, T. Onodera, T. Koda and S. Sun, *Angew. Chem., Int. Ed.*, 2008, **47**, 3588.